Inorg. Chem. **2002**, *41*, 2946–2952

Spontaneous Assembly of a Polymeric Helicate of Sodium with LVO_2 Units Forming the Strand: Photoinduced Transformation into a Mixed-Valence Product

Subodh Kanti Dutta,[†,‡] Satyabrata Samanta,[†] Suman Mukhopadhyay,[†] Pannee Burckel,[§] A. Alan Pinkerton,[§] and Muktimoy Chaudhury*[,†]

Department of Inorganic Chemistry, Indian Association for the Cultivation of Science, Kolkata 700 032, India, and Department of Chemistry, College of Arts and Sciences, The University of Toledo, Toledo, Ohio 43606-3390

Received December 27, 2001

The anionic *cis*-dioxovanadium(V) complex species LVO_2^- of a tridentate ONS ligand (H_2L) can bind sodium ion in a bis-monodentate fashion like a bridging carboxylate group. The product $[LVO_2Na(H_2O)_2]_\infty$ (**1**) is a water soluble polymeric compound in which the complementary units are held together by the simultaneous use of hydrogen bonding and Coulombic interactions. Crystallographic characterization reveals that **1** is a single stranded helicate with LVO_2^- units forming the strand which surrounds the labile sodium ions that occupy the positions on the axis. In solution of protic solvents, viz. water and methanol, **1** is quite stable as indicated by electrical conductivity and ^{1}H NMR measurements. In aprotic solvents, viz. CH_3CN, DMF, or DMSO, however, the extended hydrogen bonded network in **1** breaks apart and the helical structure collapses when irradiated with visible light. The product is a mixed-oxidation vanadium(IV/V) species obtained by photoinduced reduction as confirmed by EPR, time dependent ^{1}H NMR, and electronic spectroscopy. Compound **1** is a rare example of a nonnatural helix where hydrogen bonding interactions play a crucial role in stabilizing the single stranded polymeric structure such as that frequently observed in the biological world.

Introduction

Helicates[1] are multinuclear metal complexes in the form of molecular threads[2] with controlled and sequential turns around their axes thus generating supramolecular architectures with acquired chirality. In the biological world, molecular helicity is a common occurrence. Prime examples are α-helical polypeptides and double helical nucleic acids which play significant roles in sustaining the life process.[3,4] Understanding these natural processes at a molecular level,[1c,5] accessing new types of chiral molecules,[6] and, above all, achieving new supramolecular species with potential device applications[7] have triggered much of the recent studies on metal directed self-organization of oligomeric ligands into helical superstructures.[8−11] While hydrogen bonding, stacking

* To whom correspondence should be addressed. E-mail: icmc@mahendra.iacs.res.in.

† Indian Association for the Cultivation of Science.

‡ Present address: Department of Chemistry, Western Michigan University, Kalamazoo, MI 49008.

§ The University of Toledo.

(1) (a) Lehn, J.-M.; Rigault, A.; Seigel, J.; Harrowfield, J.; Chevrier, B.; Moras, D. *Proc. Natl. Acad. Sci. U.S.A.* **1987**, *84*, 2565. (b) Lehn, J.-M. *Angew. Chem., Int. Ed. Engl.* **1990**, *29*, 1304. (c) Koret, U.; Harding, M. M.; Lehn, J.-M. *Nature* **1990**, *346*, 339.

(2) Dietrich-Buchecker, C. O.; Sauvage, J.-P. *Chem. Rev.* **1987**, *87*, 795. (b) Sauvage, J.-P. *Acc. Chem. Res.* **1990**, *23*, 319.

(3) Bränden, C.; Tooze, J. *Introduction to Protein Structure*; Garland: New York, 1991.

(4) Saenger, W. *Principles of Nucleic Acid Structure*; Springer: New York, 1984.

(5) Schoentjes, B.; Lehn, J.-M. *Helv. Chim. Acta* **1995**, *78*, 1.

(6) (a) Maruoka, K.; Murase, N.; Yamamoto, H. *J. Org. Chem.* **1993**, *58*, 2938. (b) Evans, D. A.; Woerpel, K. A.; Scott, M. J. *Angew. Chem., Int. Ed. Engl.* **1992**, *31*, 430.

(7) (a) Anelli, P. L.; Ashton, P. R.; Ballardini, R.; Balzani, V.; Delgado, M.; Gandolfi, M. T.; Goodnow, T. T.; Kaifer, A. E.; Philp, D.; Pietraszkiewicz, M.; Prodi, L.; Reddington, M. V.; Slawin, A. M. Z.; Spencer, N.; Stoddart, J. F.; Vicent, C.; Williams, D. J. *J. Am. Chem. Soc.* **1992**, *114*, 193. (b) Balzani, V. *Tetrahedron* **1992**, *48*, 10443. (c) Slate, C. A.; Striplin, D. R.; Moss, J. A.; Chen, P.; Erickson, B. W.; Meyer, T. J. *J. Am. Chem. Soc.* **1998**, *120*, 4885. (d) Amabilino, D. B.; Ramos, E.; Serrano, J.-L.; Veciana, J. *Adv. Mater.* **1998**, *10*, 1001. (e) Cornelissen, J. J. L. M.; Fischer, M.; Sommerdijk, N. A. J. M.; Nolte, R. J. M. *Science* **1998**, *280*, 1427. (f) Zelicovich, L.; Libman, J.; Shanzer, A. *Nature* **1995**, *374*, 790.

(8) (a) Lehn, J.-M. *Supramolecular Chemistry, Concepts and Perspective*; VCH: Weinheim, 1995. (b) Lehn, J.-M. In *Perspectives in Coordination Chemistry*; Williams, A. F., Floriani, C., Merbach, A., Eds.; VCH: Weinheim, 1992; p 447.

10.1021/ic011311t CCC: $22.00
Published on Web 05/10/2002

effects, and hydrophobic interactions play key roles in the formation and stabilization of biological helices,[12] the equivalent requirements for helicate formation on the other hand are met by the stereoelectronic molecular information encoded in the preprogrammed molecular components[10] of self-assembly.[13]

Despite an extensive literature describing double and triple stranded helicates,[8−11] surprisingly little has been reported on the single stranded products.[14−20] Most reports are for compounds with Ag^+ ion on the axis,[15−18] which compare well with the structure of natural α-helices. Herein, we report an unusual type of water-soluble polymeric single stranded helicate $[LVO_2Na(H_2O)_2]_\infty$ (**1**) involving sodium ions on the axis. The *cis*-dioxo moiety of an anionic vanadium complex $[VO_2L]^-$ (H_2L = *S*-methyl 3-((2-hydroxyphenyl)methyl)-dithiocarbazate) acts as a bis-monodentate ligand to the aquated sodium ion centers, generating a polymeric structure with helical topology. The structure of this molecule both in the solid state and in solution has been examined in detail. Photochemical transformation of **1** in solution into a mixed-oxidation vanadium(IV/V) species is also established.

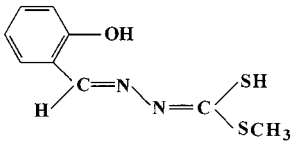

H_2L

Experimental Section

Materials. The tridentate ligand (H_2L)[21] and $[VO(acac)_2]$[22] (Hacac = acetylacetone) were prepared following published procedures. Solvents were of reagent grade and were dried from appropriate reagents[23] and distilled under nitrogen prior to use. All other chemicals were reagent grade, available commercially and used as received.

Preparation of $[LVO_2Na(H_2O)_2]_\infty$ (1). To a stirred acetonitrile solution (30 mL) of $[VO(acac)_2]$ (0.4 g, 1.5 mmol) was added an equimolar amount of the ligand H_2L (0.34 g) in the same solvent (15 mL), and the mixture was refluxed for 10 min to get a clear brown solution. To this was then added an aqueous solution (5 mL) of sodium carbonate (0.10 g), and the resulting solution was further refluxed for 1 h. The green solution obtained at this stage was filtered and the filtrate allowed to stand in the air for several days becoming gradually yellow in color. The solution was rotary evaporated to about 15 mL in volume when a yellow crystalline product slowly began to appear. It was collected by filtration, washed with methanol/Et_2O (1:1 v/v), and finally dried in vacuo. The product was recrystallized from methanol. Yield: 0.34 g (62%). Anal. Calcd for $C_9H_{12}NaN_2O_5S_2V$: C, 29.51; H, 3.28; N, 7.65; Na, 6.28. Found: C, 29.90; H, 3.29; N, 7.80; Na, 6.32%. IR (KBr disk, cm^{-1}): ν(OH) 3480, 3380(b); ν(C═N) 1600(s); ν(C═O/phenolate) 1540(s); ν (V═O_t) 970, 900 (s). UV−vis (CH_3OH) [λ_{max}, nm (ϵ, M^{-1} cm^{-1})]: 393 (8200), 290 (26100), 230 (31500).

Physical Measurements. EPR spectra in solution were recorded in the X-band on a Bruker model ESP 300E spectrometer. Electronic spectra in the near-IR region were obtained on a Hitachi U-3400 UV−vis−NIR spectrometer. The ^{1}H NMR spectra were recorded on a Bruker model Avance DPX 300 spectrometer. Solution electrical conductivity and IR and UV−vis spectra were obtained as described elsewhere.[24] pH measurements were made with a Systronics model 335 digital pH meter. Cyclic voltammetry in solution was performed with a PAR model 362 scanning potentiostat using Pt working and auxiliary electrodes. A saturated calomel electrode (SCE) was used for reference, and ferrocene, as internal standard.[25] Solutions were ~10^{-3} M in samples and contained 0.1 M TEAP as the supporting electrolyte.

Elemental analyses (for C, H, and N) were performed in this laboratory (at IACS) using a Perkin-Elmer 2400 analyzer. Sodium contents were estimated using a Thermo Jarrell Ash (Model Atom Scan 16) inductively coupled plasma atomic absorption spectrometer.

X-ray Crystallography. Diffraction quality crystals of **1** were grown at room temperature by slow evaporation from a methanol−water (1:1 v/v) solution of the compound. A clear yellow elongated plate with dimensions 0.40 × 0.30 × 0.05 mm^3 was mounted on a glass fiber and used for data collection at 21 ± 1 °C in $\omega-2\theta$ scan mode on an Enraf-Nonius CAD-4 diffractometer equipped with graphite monochromatized Mo Kα (λ = 0.71073 Å) radiation. The background was obtained from an analysis of the scan profile.[26] No crystal decay was observed during the data collection. The unit cell parameters were obtained by least-squares refinement of the angular settings for 25 reflections in the 2θ range of 24°−28°. Relevant crystallographic data are given in Table 1. Selected bond lengths, bond angles, and hydrogen bond geometry are given in Table 2.

Data were corrected for Lorentz and polarization effects. An empirical absorption (from 0.762 to 1.000 on *I*) correction was also applied. The maximum 2θ value for data collection was 52.0°. The number of measured reflections was 3184, and of these, 2393 unique reflections, which satisfied the $F_o^2 \geq 3.0\sigma(F_o^2)$ criterion, were used for structure solution. The structure was solved by direct methods

(9) (a) Constable, E. C. In *Comprehensive Supramolecular Chemistry*; Sauvage, J.-P.; Hosseini, M. W., Eds.; Pergamon: Oxford, 1996; Vol. 9. (b) Constable, E. C. *Chem. Ind. (London)* **1994**, 56. (c) Constable, E. C. *Prog. Inorg. Chem.* **1994**, *42*, 67.
(10) Piguet, C.; Bernardinelli, G.; Hopfgartner, G. *Chem. Rev.* **1997**, *97*, 2005.
(11) Williams, A. F. *Chem.−Eur. J.* **1997**, *3*, 15.
(12) Meurer, K. P.; Vögtle, F. In *Topics in Current Chemistry*; Boschke, F. L., Ed.; Springer-Verlag: Berlin, 1985; Vol. 127, pp 1−76.
(13) (a) Lindsey, J. S. *New. J. Chem.* **1991**, *15*, 153. (b) Philp, D.; Stoddart, J. F. *Angew. Chem., Int. Ed. Engl.* **1996**, *35*, 1154.
(14) Erxleben, A. *Inorg. Chem.* **2001**, *40*, 412.
(15) Carlucci, L.; Ciani, G.; Prosserpio, D. M.; Sironi, A. *Inorg. Chem.* **1998**, *37*, 5941.
(16) Withersky, M. A.; Blake, A. J.; Champness, N. R.; Hubberstey, P.; Li, W.-S.; Schröder, M. *Angew. Chem., Int. Ed. Engl.* **1997**, *36*, 2327.
(17) Wu, B.; Zhang, W.-J.; Yu, S.-Y.; Wu, X.-T. *J. Chem. Soc., Dalton Trans.* **1997**, 1795.
(18) Suzuki, T.; Kotsuki, H.; Isobe, K.; Moriya, N.; Nakagawa, Y.; Ochi, M. *Inorg. Chem.* **1995**, *34*, 530.
(19) Gelling, O. J.; van Bolhuis, F.; Feringa, B. L. *J. Chem. Soc., Chem. Commun.* **1991**, 917.
(20) Cathey, C. J.; Constable, E. C.; Hannone, M. J.; Tocher, D. A.; Ward, M. D. *J. Chem. Soc., Chem. Commun.* **1990**, 621.
(21) Dutta, S. K.; Tiekink, E. R. T.; Chaudhury, M. *Polyhedron* **1997**, *16*, 1863.
(22) Rowe, R. A.; Jones, M. M. *Inorg. Synth.* **1957**, *5*, 113.
(23) Perrin, D. D.; Armarego, W. L. F.; Perrin, D. R. *Purification of Laboratory Chemicals*, 2nd ed.; Pergamon: Oxford, England, 1980.
(24) (a) Dutta, S. K.; Kumar, S. B.; Bhattacharyya, S.; Tiekink, E. R. T.; Chaudhury, M. *Inorg. Chem.* **1997**, *36*, 4954. (b) Dutta, S. K.; McConville, D. B.; Youngs, W. J.; Chaudhury, M. *Inorg. Chem.* **1997**, *36*, 2517. (c) Bhattacharyya, S.; Ghosh, D.; Mukhopadhyay, S.; Jensen, W. P.; Tiekink, E. R. T.; Chaudhury, M. *J. Chem. Soc., Dalton Trans.* **2000**, 4677.
(25) Gagné, R. R.; Koval, C. A.; Lisensky, G. C. *Inorg. Chem.* **1980**, *19*, 2854.
(26) Blessing, R. H.; Coppens, P.; Becker, P. *J. Appl. Crystallogr.* **1974**, *7*, 488.

Table 1. Summary of Crystallographic Data

empirical formula	$C_9H_{12}NaN_2O_5S_2V$
fw	366.27
space group	monoclinic, $P2_1/c$ (No. 14)
a, Å	16.005(2)
b, Å	6.142(1)
c, Å	14.728(3)
β, deg	101.03(1)
V, Å^3	1421(1)
Z	4
T, °C	21 ± 1 °C
λ(Mo Kα), Å	0.71073
ρ_{calcd}, g cm^{-3}	1.71
μ, mm^{-1}	1.04
R^a (R_w^b)	0.029 (0.085)

^{a} $R = \sum(||F_o| - |F_c||)/\sum |F_o|$. ^{b} $R_w = [\sum w(||F_o| - |F_c||)^2/\sum w|F_o|^2]^{1/2}$.

Table 2. Selected Bond Distances and Angles for $[LV^VO_2Na(H_2O)_2]_\infty$ (**1**)

		Distances (Å)	
V−O(1)	1.648(2)	N(1)−C(3)	1.291(3)
V−O(2)	1.613(2)	Na−O(1)	2.406(2)
V−O(3)	1.911(2)	Na−O(2)^b	2.380(2)
V−S(1)	2.3764(9)	Na−O(4)	2.381(2)
V−N(1)	2.178(2)	Na−O(5)	2.357(2)
C(1)−S(1)	1.735(2)	Na−O(5)^b	2.415(2)
N(1)−N(2)	1.409(2)	Na−S(1)^a	3.177(1)
Na Na^b	4.000(2)		
		Angles (deg)	
S(1)−V−O(1)	87.85(6)	O(1)−Na−O(5)	93.37(7)
S(1)−V−O(2)	104.79(7)	O(1)−Na−S(1)^a	84.80(5)
S(1)−V−O(3)	145.86(5)	O(4)−Na−O(5)^b	87.40(7)
S(1)−V−N(1)	76.72(5)	O(4)−Na−O(2)^b	100.92(7)
O(1)−V−O(2)	108.56(8)	O(4)−Na−O(5)	166.40(7)
O(1)−V−O(3)	96.65(7)	O(4)−Na−S(1)^a	85.47(6)
O(1)−V−N(1)	150.72(7)	O(5)^b−Na−O(2)^b	83.95(7)
O(2)−V−O(3)	105.72(8)	O(5)^b−Na−O(5)	106.07(6)
O(2)−V−N(1)	99.45(8)	O(5)^b−Na−S(1)^a	166.56(6)
O(3)−V−N(1)	83.49(6)	O(2)^b−Na−O(5)	82.81(7)
O(1)−Na−O(4)	86.13(7)	O(2)^b−Na−S(1)^a	108.58(5)
O(1)−Na−O(5)^b	83.37(6)	O(5)−Na−S(1)^a	80.95(5)
O(1)−Na−O(2)^b	165.19(6)	V−O(1)−Na	125.98(8)

Hydrogen Bond Geometry

D−H···A	D···H, Å	H···A, Å	D···A, Å	D−H···Å, deg
O(4)−H(42)···O(1)^c	0.83(3)	2.03(3)	2.827(3)	160(3)
O(5)−H(51)···O(4)^d	0.78(3)	2.06(3)	2.812(3)	163(3)
O(5)−H(52)···O(3)^e	0.68(4)	2.29(4)	2.937(3)	161(4)

^{a} $-x, -y, -z$. ^{b} $-x, y + 1/2, -z + 1/2$. ^{c} $-x, -y + 1, -z$. ^{d} $x, y - 1, z$. ^{e} $-x, y - 1/2, -z + 1/2$.

(MULTAN 80)[27] and refined by a full-matrix least-squares procedure minimizing the function $\sum\omega(|F_o| - |F_c|)^2$, where $\omega = 1/[\sigma^2(F_o^2) + (0.0564P)^2 + 0.3361P]$ and $P = (F_o^2 + 2F_c^2)/3$. Scattering factors for neutral atoms and the values for $\Delta f'$ and $\Delta f''$ were taken from the usual sources.[28] Non-hydrogen atoms were refined with anisotropic thermal parameters, and hydrogen atoms were included in the models in their calculated positions (C−H, 0.97 Å). The refinements were continued until convergence employing σ weights. Final R and R_w values are 0.029 and 0.085, respectively, and the goodness of fit (S) = 1.108 for 229 refined parameters. The final Fourier difference synthesis showed a maximum and minimum of +0.41(6) and −0.26(6) e/Å^3. Structure refinements were performed by using SHELXL-97.[29] The molecular structures and atom-labeling scheme shown in Figures 1−3 were drawn by Bruker SHELXTL package.

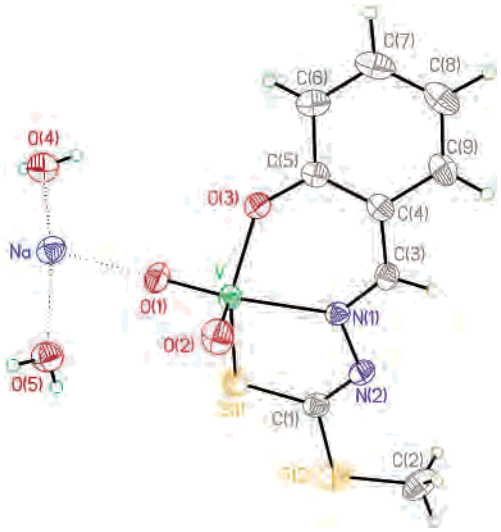

Figure 1. Molecular structure for the complex $[LVO_2Na(H_2O)_2]_\infty$ (**1**) showing the atom numbering (50% probability ellipsoids).

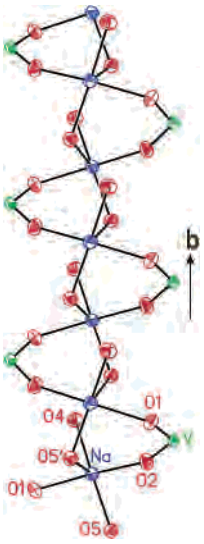

Figure 2. Drawing of the helicate (**1**) viewed parallel to the *b*-axis.

Photochemical Study. A clear yellow solution of **1** in acetonitrile was placed in a quartz cell and purged with purified dinitrogen for 20 min. A tungsten filament lamp (60 W) was used as a visible light source to irradiate this solution which gradually turned green during photolysis. The green solutions obtained after different intervals of exposure time were used for subsequent characterization. Reported pH values in acetonitrile solutions are uncorrected.

Results and Discussion

Synthesis. Complex **1** is prepared by the reaction of [VO(acac)$_2$] with a stoichiometric (1:1 mol ratio) amount of the ligand H_2L in aqueous acetonitrile medium in the presence of sodium carbonate. The obligatory steps in this preparative procedure are the presence of water in the reaction mixture and its subsequent exposure to atmospheric oxygen as

(27) Main, P.; Fiske, S. J.; Hull, S. E.; Lessinger, L.; Germain, G.; Declerq, J. P.; Wollfson, N. M. MULTAN 80, University of York, England, 1980.

(28) *International Tables for X-ray Crystallography*; Kynoch Press: Birmingham, England, 1974; Vol. IV; present distributor, Kluwer Academic Publishers: Dordrecht, The Netherlands.

(29) Sheldrick, G. M. *SHELXL-97*; University of Göttingen: Göttingen, Germany, 1997.

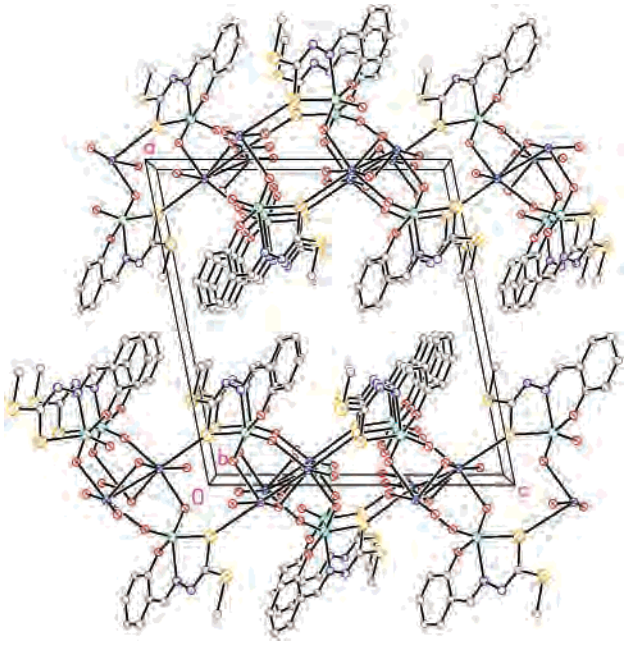

Figure 3. Packing diagram of **1** viewed down the *b*-axis showing the linking of the helices into layers.

confirmed by several control experiments. The product is a single stranded helix $[LVO_2Na(H_2O)_2]_\infty$ with an infinite polymeric structure containing an alternating array of *cis*-dioxo vanadium(V) $[LVO_2^-]$ units and aquated sodium ion centers, as confirmed by X-ray crystallography (see later). An identical procedure using tetraethylammonium ion as replacement for sodium affords an intractable material of unknown composition. Interestingly, the present molecule offers a rare example[30] where sodium ions form the axis of a helicate. The bent LVO_2^- unit with a formal negative charge on it binds the aquated sodium ion in a bis-monodentate manner to generate the infinite helical strand. The complementary units in **1** are thus held together by the process of self-assembly through the simultaneous use of hydrogen bonding and Coulombic interactions. Similar bonding interactions have been used systematically in crystal engineering to generate organic supramolecular compounds.[31]

The IR spectrum of **1** contains all the pertinent bands of the coordinated tridentate ligand (L^{2-}) as discussed earlier.[24a,32] In addition, a strong two-band pattern is observed at 970 and 900 cm^{-1}, characteristic of a *cis*-dioxovanadium moiety.[33] In the high-frequency region, a sharp medium intensity band at 3530 cm^{-1}, coupled with two broad absorptions at 3480 and 3380 cm^{-1}, indicates the presence of coordinated water in the molecule.

Description of the Crystal Structure. The molecular structure of **1** is shown in Figure 1. Important interatomic parameters are listed in Table 2. The molecule when viewed along the *b*-axis exhibits an infinite spiral of ···O···V···O···Na···O··· chain as shown in Figure 2. Individual vanadium(V) centers exist in a distorted square pyramidal geometry (Figure 1), with the four basal positions from the tridentate ligand and one of the terminal oxo ligands O(1) of the *cis*-VO_2 core. The axial site is occupied by the remaining oxo ligand O(2) which forms angles in the range 99.45(8)°−108.56(8)° with the basal plane. The angles O(3)−V−S(1) and O(1)−V−N(1) are 145.86(5)° and 150.72(7)°, respectively, which indicate that the central vanadium atom is shifted slightly (0.5097(8) Å) out of the basal plane toward the apical oxygen O(2) atom. The O(1)−V−O(2) angle (108.56(8)°) and the terminal V═O distances (1.648(2) and 1.613(2) Å) are in the expected range.[33]

An intriguing structural feature of this compound is the presence of hexacoordinated sodium ion centers, each acting as a bridge between the two neighboring LVO_2 moieties. As shown in Figure 2, each LVO_2 moiety in turn is bound to two adjacent sodium ions through terminal oxo ligands, thus forming an infinite helicate with a single strand of alternating Na ions and LVO_2 moieties, and there are two of these units in each turn (along the 2_1 axis). The Na···Na distance between the immediate neighbors is 4.000(2) Å. Besides the terminal oxo ligands, each sodium ion also has two types of water molecule in its coordination sphere. One is exclusively attached to a single sodium ion as denoted by O(4), and the other, denoted by O(5), occupies a bridging position between the two adjacent sodium ions. Thus, two vanadyl oxo atoms O(2) and O(1)′ from two different vanadyl centers and an oxygen atom O(5)′ from a bridging water molecule constitute three atoms of the equatorial plane, while the apical sites are occupied by O(4) and O(5) oxygen atoms (O(4)−Na−O(5), 166.40(7)°) of a nonbridging and bridging water molecule. The sixth coordination site is occupied by S(1) from a neighboring helicate strand, thus linking the helicates into a layer perpendicular to *a*. In this manner, the structure may be described as hydrophilic layers separated by hydrophobic layers due to the organic moieties (Figure 3). There are several secondary interactions in this molecule, viz. between O(1)−O(4), O(5)−O(3), and O(5)−O(4) atoms, all through strong hydrogen bonds as listed in Table 2. These hydrogen bonding interactions play a major role in stabilizing this unusual helical structure. Very few helicate molecules[34−36] are known in which hydrogen bonding exerts such a delicate influence such as is observed in biological helices.

Structure in Solution. A solution of **1** in water or methanol is stable for several days and shows feeble conductivity (Λ_M in water is 20 Ω^{-1} cm^2 mol^{-1}), giving a clear indication that the sodium ions remain coordinated in solution. Addition of an equivalent amount of benzo-15-crown-5 ether does not make any notable difference in the electrical conductivity of the solution.

^{1}H NMR Spectroscopy. ^{1}H NMR data for **1** in various solvents along with those of the free ligand H_2L in acetone-d_6 are summarized in Table 3. The free ligand has a broad resonance at 10.93 ppm due to a phenolic OH proton which

(30) Bell, T. W.; Jousselin, H. *Nature* **1994**, *367*, 441.
(31) Félix, O.; Hosseini, M. W.; De Cian, A.; Fischer, J. *Angew. Chem., Int. Ed. Engl.* **1997**, *36*, 102.
(32) Dutta, S. K.; Samanta, S.; Kumar, S. B.; Han, O. H.; Burckel, P.; Pinkerton, A. A.; Chaudhury, M. *Inorg. Chem.* **1999**, *38*, 1982.
(33) Li, X.; Lah, M. S.; Pecoraro, V. L. *Inorg. Chem.* **1988**, *27*, 4657.
(34) Ezuhara, T.; Endo, K.; Aoyma, Y. *J. Am. Chem. Soc.* **1999**, *121*, 3279.
(35) Batten, S. R.; Hoskins, B. F.; Robson, R. *Angew. Chem., Int. Ed. Engl.* **1997**, *36*, 636.
(36) Libman, J.; Tor, Y.; Shanzer, A. *J. Am. Chem. Soc.* **1987**, *109*, 5880.

Table 3. ^{1}H NMR Spectral Data (δ, ppm)[a] for the Free Ligand (H_2L) and Complex **1** at 23 °C

H_2L/acetone-d_6	**1**/MeOD-d_4	**1**/DMSO-d_6	**1**/MeCN-d_3	assignment[b]
10.93 bs				1H, phenolic OH
8.51 s	8.98 s	9.01 s	8.95 s	1H, H^3
7.48 d (6.6)	7.58 d (7.5)	7.64 d (7.6)	7.55 d (7.5)	1H, H^6
7.40 t (11.4)	7.44 t (7.6)	7.40 t (8.5)	7.42 t (7.7)	1H, H^8
7.00 m	6.97 m	6.64 m	6.93 m	2H, H^9, H^7
	4.60 s	3.40 s	2.28 s	H_2O/HOD
2.65 s	2.59 s	2.54 s	2.57 s	3H, SCH_3

[a] Chemical shifts are relative to internal TMS at 0 ppm: b, broad; s, singlet; d, doublet; t, triplet; m, multiplet. Values in the parentheses represent coupling constants (J in Hz). [b] Proton labels are as shown in Figure 1.

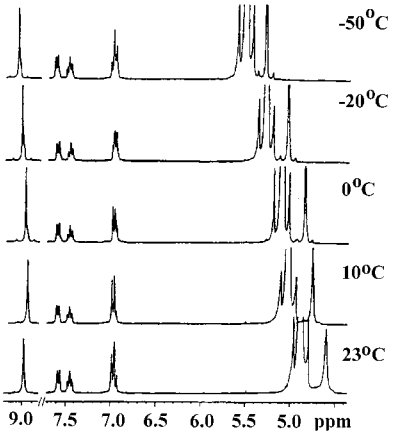

Figure 4. Variable temperature 300 MHz ^{1}H NMR spectra of **1** (δ, 4.4−9.1 ppm region) in methanol-d_4.

is missing in the complex. The spectrum of **1** is relatively straightforward, practically independent of solvent, except the protons due to aqua ligands which appear as a singlet in the range 4.60−2.28 ppm at room temperature (23 °C) depending upon the dielectric of the solvent. Both azomethine (H^3, ∼9.00 ppm)[37] and phenyl ring (H^6, ∼7.6 ppm) protons in **1** are shifted downfield compared to those in the free ligand, thus indicating participation of phenolate oxygen and imino nitrogen in metal coordination confirming the results of X-ray crystallography. In methanol-d_4, the spectrum of **1** remains virtually unchanged in the temperature range 23 to −50 °C (Figure 4), excepting the singlet due to coordinated water molecules which appears at 4.6 ppm (at 23 °C) and shows a gradual downfield shift with the lowering of temperature. The results clearly indicate that compound **1** retains its structural identity in solution over the temperature range of our study.

In dry aprotic solvents, viz. acetonitrile, DMF, or DMSO, fresh yellow solutions of **1** gradually turn green with exposure to visible light. Progress of the photochemical reaction in CH_3CN was followed by ^{1}H NMR experiments. The results are displayed in Figure 5 which reveals gradual loss of resolution as well as line broadening of the main spectral features with an increase in exposure time. The results indicate generation of a paramagnetic species by reduction through a photochemical pathway as confirmed by control experiments.

(37) Proton labels are as shown in Figure 1.

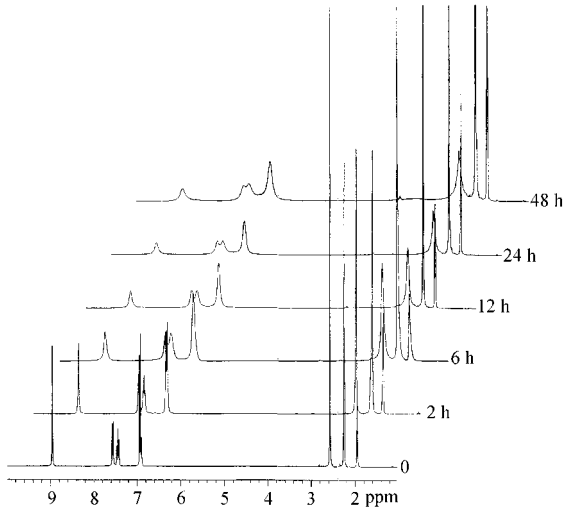

Figure 5. Time-dependent ^{1}H NMR spectra of **1** in acetonitrile-d_3 solution under the exposure of visible light, showing gradual line broadening.

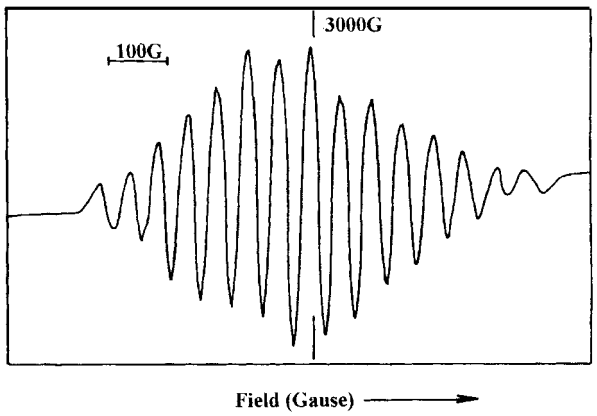

Figure 6. X-band EPR spectrum of a photoreduced solution of **1** in acetonitrile at room temperature.

Identification of the Photoreduced Product. Despite our best effort, we were unable to isolate the green paramagnetic photoreduced product (**2**) in the solid state. In solution, however, compound **2**, unlike its precursor, is EPR active, providing a fifteen-line spectrum at room temperature (Figure 6) with $<g> = 2.136$. This indicates generation of a species involving a coupled vanadium ($I = {}^7/_2$) center with an odd interacting electron. The hyperfine splitting parameter $<A>_{15}$, 48.4×10^{-4} cm^{-1} in this case, is almost half of that of a localized spectrum ($<A>_8$, 89×10^{-4} cm^{-1}) reported earlier[32] for a μ-oxo divanadium(IV/V) compound with closely similar ligands. This observation again speaks in favor of **2** to be a dinuclear species[38] with mutually interacting vanadium(IV/V) centers.

As mentioned in the Experimental Section, a freshly prepared solution of **1** in acetonitrile is optically transparent in the near-IR−visible region. The green photoreduced solution however absorbs in the 1300−500 nm range, generating a broad, well developed band of moderately high intensity at 970 nm along with a low intensity shoulder centered at 710 nm, A_{970}/A_{710} being close to 1.60 after a 12 h exposure time (Figure 7). While the near-IR band (at 970

(38) Slichter, C. P. *Phys. Rev.* **1955**, *99*, 478.

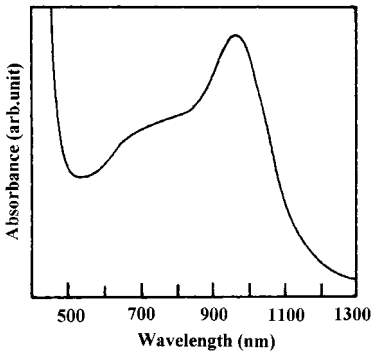

Figure 7. Vis−NIR electronic absorption spectrum of a photoreduced solution of **1** ($\sim 1.0 \times 10^{-3}$ M) in acetonitrile after 12 h exposure to visible light.

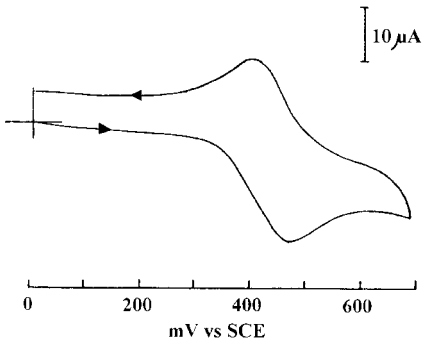

Figure 8. Cyclic voltammogram of a photoreduced solution of **1** in acetonitrile (exposure time 12 h); potential vs SCE, 0.1 M TEAP at a platinum electrode, scan rate 50 mV s^{-1}.

nm), on the basis of its shape and intensity, is anticipated as arising from an intervalence transfer (IT) transition, the absorption in the visible region (at 710 nm) is more likely to have a ligand-field origin localized on an oxovanadium-(IV) center.[24a]

Another important piece of evidence toward identification of the photoreduced product (**2**) comes from the cyclic voltammetric study. Although the precursor compound **1** is electrochemically inactive, **2** in acetonitrile solution, when examined by cyclic voltammetry, displays (Figure 8) a reversible one-electron oxidation at $E_{1/2} = 0.44$ V versus SCE (ΔE_p, 70mV; i_{pa}/i_{pc}, 0.93). The electrochemical results thus indicate the presence of an oxidizable vanadium(IV) center in **2** as established by EPR experiments.

Recently, we have been successful in synthesizing mixed-oxidation divanadium(IV/V) compounds[24a,32] containing a $V_2O_3^{3+}$ core with the same and related ligands. One of these compounds, (BzImH) [$LOV^{IV}-O-V^{V}OL$] (BzIm = benzimidazole), **3**, with the same ONS donor ligand as in **1**, has been structurally characterized.[24a] Some of the relevant physicochemical data for **3** are displayed in Table 4 along with those of compound **2** for a direct comparison. The observed similarities strongly suggest the generation of a mixed-oxidation divanadium(IV/V) compound during photoinduced reduction of **1** in dry aprotic solvents.

Proton-Coupled Photoreduction. The $V{=}O_t$ terminal oxygen atoms in **1** are all coordinated to sodium ions predominantly by noncovalent interactions. When **1** is dissolved in aprotic solvents of high donor capacity, the solvent molecules possibly compete and replace the coordinated water molecules from the metal coordination sphere with concomitant break down of the hydrogen bonding network,[39] responsible for the stability of the helical structure. As the helical structure falls apart, the terminal oxygen atoms of LVO_2^- units are now available for protonation[40] to generate vanadyl ($LV^{IV}O$) species by a photoreduction process that probably involves the intermediate formation of a hydroxo species[33,41,42] (eqs 1 and 2).

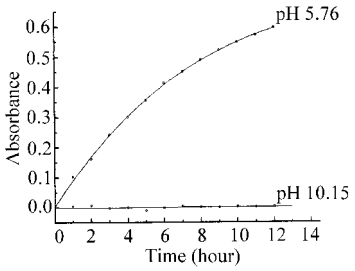

Figure 9. Time evolution of an intervalence charge transfer band at 970 nm due to photoinduced reduction of **1** in acetonitrile at pH 5.76 and 10.15.

Table 4. Comparison between the Physical Characteristics and Spectroscopic and Electrochemical Features of Compound **3** and the Photoreduced Product **2**

characteristics	compound **3**	photoreduced product **2**
solution color	green	green
EPR features at room temperature	15-line $\langle g \rangle = 2.128$ $\langle A \rangle \times 10^4 = 44$ cm^{-1}	15-line $\langle g \rangle = 2.136$ $\langle A \rangle \times 10^4 = 48.4$ cm^{-1}
intervalence transfer (IT) band in CH_3CN	970 nm	970 nm
cyclic voltammetric feature ($E_{1/2}$ vs SCE) in CH_3CN	0.42 V	0.44 V

$$LV^{V}O_2^- + H^+ \rightleftharpoons LV^{V}O(OH) \quad (1)$$

$$LV^{V}O(OH) + H^+ + e^- \overset{h\nu}{\rightleftharpoons} LV^{IV}O + H_2O \quad (2)$$

$$LV^{IV}O + LV^{V}O_2^- \rightleftharpoons [LV^{IV}O-(\mu\text{-}O)-OV^{V}L]^- \quad (3)$$

$LV^{IV}O$ thus produced reacts with excess $LV^{V}O_2^-$ to generate the green mixed-oxidation divanadium(IV/V) product [$LV^{IV}O-(\mu$-O)$-OV^{V}L]^-$ (**2**) (eq 3). We are, however, at this stage, not quite sure about the identity of the oxidized species involved in the reaction (eq 2). A structurally characterized mixed-oxidation polyoxovanadate(IV/V) prepared by photochemical reduction has been reported recently.[43]

The intervalence charge transfer band displayed by **2** at 970 nm was used to monitor the progress of the reactions at pH 5.76 and 10.15 as displayed in Figure 9. The results show involvement of proton for the satisfactory progress of this reaction.

(39) (a) Rebek, J., Jr. *Angew. Chem., Int. Ed. Engl.* **1990**, *29*, 245. (b) Whitesides, G. M.; Mathias, J. P.; Seto, C. T. *Science* **1991**, *254*, 1312. (c) Fan, E.; Van Arman, S. A.; Kincaid, S.; Hamilton, A. J. *J. Am. Chem. Soc.* **1993**, *115*, 369.
(40) Dewey, T. M.; Du Bois, J.; Raymond, K. N. *Inorg. Chem.* **1993**, *32*, 1729.
(41) Root, C. A.; Hoeschele, J. D.; Cornman, C. R.; Kampf, J. W.; Pecoraro, V. L. *Inorg. Chem.* **1993**, *32*, 3855.
(42) Asgedom, G.; Sreedhara, A.; Kivikoski, J.; Kolehmainen, E.; Rao, C. P. *J. Chem. Soc., Dalton Trans.* **1996**, 93.
(43) Yamase, T. *J. Chem. Soc., Dalton Trans.* **1997**, 2463.

Concluding Remarks

Attempts have been made in recent times to compare certain oxovanadium species as "inorganic analogues of organic functionalities" because of some structural and chemical properties they have in common.[44] The role of LVO_2^- species here is a case in point where the *cis*-dioxovanadium(V) moiety behaves like an analogue of a bridging carboxylate group, holding the adjacent sodium ions together to form an "inorganic helix" of extended structure with a peripheral organic moiety. The reported compound is a rare example where hydrogen bonding plays a central role in stabilizing a single stranded structure of a nonnatural helix with labile sodium ion centers occupying the axis. In aprotic solvents of higher donor capacity, this unique hydrogen bonded helical structure collapses when compound **1** is irradiated with visible light. The putative product is a mixed-oxidation coupled vanadium(IV/V) species with a delocalized electronic structure on the time scale of EPR spectroscopy.

Acknowledgment. We are grateful to the Council of Scientific and Industrial Research, New Delhi, for financial support. We also thank Professor K. Nag for many useful discussions.

Supporting Information Available: X-ray crystallographic file in CIF format. This material is available free of charge via the Internet at http://pubs.acs.org.

IC011311T

(44) Giacomelli, A.; Floriani, C.; DeSouza Duarte, A. O.; Chiesi-villa, A.; Guastini, C. *Inorg. Chem.* **1982**, *21*, 3310.